Doppler tomography of the Little Homunculus: High resolution spectra of [Fe II] $\lambda 16435$ around Eta Carinae*

Nathan Smith†‡

Center for Astrophysics and Space Astronomy, University of Colorado, 389 UCB, Boulder, CO 80309, USA

Accepted 0000, Received 0000, in original form 0000

ABSTRACT

High-resolution spectra of [Fe II] $\lambda 16435$ around η Carinae provide powerful diagnostics of the geometry and kinematics of the "Little Homunculus" (LH) growing inside the larger Homunculus nebula. The LH expansion is not perfectly homologous: while low-latitudes are consistent with linear expansion since 1910, the polar caps imply ejection dates around 1920–1930. However, the expansion speed of the LH is much slower than the post-eruption wind, so the star's powerful wind may accelerate the LH. With an initial ejection speed of 200 km s⁻¹ in 1890, the LH would have been accelerated to its present speed if the mass is roughly 0.1 M_{\odot} . This agrees with an independent estimate of the LH mass based on its density and volume. In any case, an ejection after 1930 is ruled out. Using the LH as a probe of the 1890 event, then, it is evident that its most basic physical parameters (total mass and kinetic energy; $0.1 M_{\odot}$ and $10^{46.9}$ ergs, respectively) are orders of magnitude less than during the giant eruption in the 1840s. Thus, the ultimate energy sources were different for these two events – yet their ejecta have the same bipolar geometry. This clue may point toward a collimation mechanism separate from the underlying causes of the outbursts.

Key words: circumstellar matter — ISM: jets and outflows — stars: individual: η Car — stars: mass loss — stars: winds, outflows

1 INTRODUCTION

The Homunculus nebula around η Carinae is a key object for understanding bipolar mass-loss in the late stages of stellar evolution. The $\gtrsim 10~{\rm M}_\odot$ it contains (Smith et al. 2003b) constitutes the major product of η Car's giant eruption in the 1840s (Currie et al. 1996; Smith & Gehrz 1998; Morse et al. 2001). However, the process that focussed the prolate mass loss remains uncertain, even though several ideas have been pursued (e.g., Frank et al. 1995, 1998; Garcia-Segura et al. 1997; Owocki & Gayley 1997; Dwarkadis & Balick 1998; Langer et al. 1999; Maeder & Desjacques 2001; Smith 2002b; Smith et al. 2003a; Gonzalez et al. 2004; Soker 2004; Matt & Balick 2004). In this regard, the geometry of subsequent ejecta inside the Homunculus may provide critical clues.

Ishibashi et al. (2003) discovered a smaller nebula called the "Little Homunculus", revealed by Doppler shifts of narrow lines in spectra of η Car. This smaller homuncule gestating inside the larger one defies the putative gender neutrality of the Homunculus, but offers an important clue to the mechanism that caused its bipolar shape. Ishibashi et al. measured proper motions of the Little Homunculus (LH hereafter), indicating an age of roughly 100 years. The observed expansion of the LH (much slower than the Homunculus) is similar to absorption velocities seen in historical spectra from 1893 (Walborn & Liller 1977; Whitney 1952). Thus, the LH is most likely the product of a separate event, but shares the same prolate geometry as the larger Homunculus. Whatever the cause of η Car's bipolarity may be, it is persistent. There are other hints of recurring outflow geometry (Smith et al. 2004b), including the present-day bipolar wind (Smith et al. 2003a). Other ejecta have been attributed to η Car's 1890 outburst as well (Smith & Gehrz 1998; Davidson et al. 2001; Smith et al. 2004b), adding weight to the LH's putative origin in that event (but see Dorland et al. 2004).

The LH is not seen in direct visual-wavelength images because it is overwhelmed by starlight scattered off dust in the Homunculus, while emission from the LH is also obscured by that dust. However, some emission structures in-

^{*} Based on observations obtained at the Gemini Observatory, which is operated by AURA, under a cooperative agreement with the NSF on behalf of the Gemini partnership: the National Science Foundation (US), the Particle Physics and Astronomy Research Council (UK), the National Research Council (Canada), CONICYT (Chile), the Australian Research Council (Australia), CNPq (Brazil), and CONICET (Argentina).

[†] Email: nathans@casa.colorado.edu

[‡] Hubble Fellow

side the Homunculus can be recognized by their temporal variability or wavelength dependence (Smith et al. 2000, 2004a, 2004b); the "Purple Haze" and emission knots seen in [S III] and [N II] may be parts of the LH.

Fortunately, the LH exhibits very bright emission from infrared (IR) lines of [Fe II], most notably [Fe II] $\lambda 16435$ (Smith 2002b). This line can be enhanced in shocks or photodissociation regions, and bright [Fe II] $\lambda 16435$ is common in nebulae of other luminous blue variables (Smith 2002a). The high-resolution spectra of [Fe II] $\lambda 16435$ presented here significantly advance our understanding of the kinematics of the LH. They have higher dispersion and better sensitivity than earlier data, and the infrared [Fe II] line can more easily penetrate the intervening dust screen.

Although thermal-IR images do not show the LH, presumably due to insufficient dust, they have revealed a bright dust torus, marking the point in the equator where the two lobes of the Homunculus meet (Smith et al. 2002, 2003b). Since this dust torus and the LH both occupy similar projected areas on the sky (within $\sim\!\!2''$ of the star), the relationship between them is ambiguous. Using [Fe II] $\lambda 16435$ emission to compare the spatial extents of the LH and dust torus is one goal of this paper, in addition to constraining other properties of the LH and the 1890 outburst.

2 OBSERVATIONS

The 0″.34-wide long-slit aperture was oriented at P.A.=310° along the polar axis of the Homunculus (Fig. 1). To sample the kinematics across the LH, the slit was positioned on the bright central star, plus offsets of 1″ and 2″ in either direction perpendicular to the slit axis as shown in Fig. 1. At each slit position, three pairs of 60-second exposures sampled [Fe II] 16435, for a total on-source exposure time in middle regions of the Homunculus of 6 min.

HR 5571 was observed with Phoenix on the same night with the same grating setting in order to correct for telluric absorption. Telluric lines were used for wavelength calibration, using the telluric spectrum available from NOAO. Velocities were calculated adopting a vacuum rest wavelength of 16439.981 Å for the [Fe II] $\lambda 16435~(a^4F-a^4D)$ line, and these velocities were corrected to a heliocentric reference frame. (Heliocentric velocities will be quoted here.) Uncertainty in the resulting velocities is $\pm 1~{\rm km~s}^{-1}$, dominated by scatter in the dispersion solution for telluric lines.

Figure 2 shows the resulting long-slit data for [Fe II] at the five different slit positions, where the bright reflected continuum light in the Homunculus has been subtracted out to enhance the contrast of the line emission. Structures near the center of each panel (at $\pm 250~\rm km~s^{-1}$) are from the LH, while filaments from the Homunculus are seen at larger velocities (see Smith 2002b). The vertical dashed lines in Fig. 1 mark the systemic velocity of η Car at $-8.1~\rm km~s^{-1}$, mea-

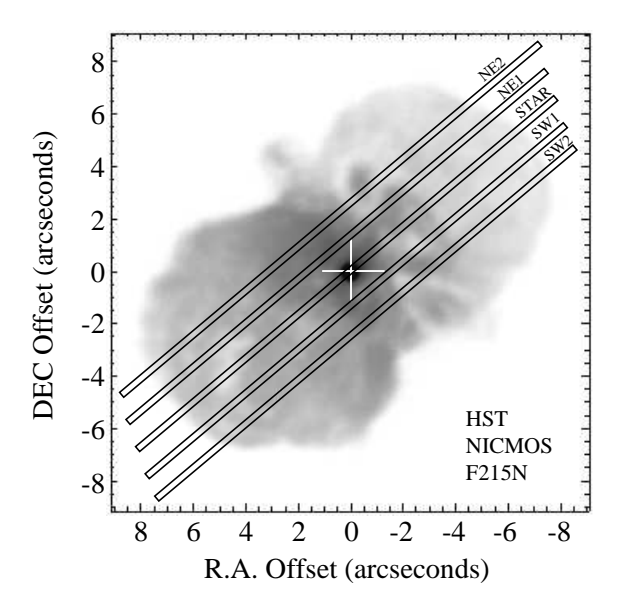


Figure 1. Phoenix slit aperture positions superposed on a 2 μ m HST/NICMOS image of η Car from Smith & Gehrz (2000).

sured from earlier Phoenix spectra of H_2 in the Homunculus (Smith 2004). The H_2 systemic velocity is more reliable than that given by narrow $H\alpha$ emission (Boumis et al. 1998), because of asymmetric and variable ionization structure in ejecta near the star (e.g., Smith et al. 2004a, 2004b).

3 KINEMATIC STRUCTURE

With a few exceptions due to extinction (see below), all five slit positions in Figure 2 confirm the basic bipolar structure inferred by Ishibashi et al. (2003). In general, the LH is a miniature version of the larger Homunculus, although the general shape appears more scrunched in the polar direction. In every case the polar cap on the blueshifted lobe is clearly seen, while it was harder to discern in earlier data at visual wavelengths (Ishibashi et al. 2003). Thus, the star's much faster stellar wind has not yet cleared a path through the slower LH; such resistance by the LH may have important consequences for its mass, momentum, and acceleration (see §4 and §6). However, in general, [Fe II] emission in Figure 2 gives the impression that the LH is clumpy, with a filling factor of perhaps 0.5. The five slit placements sampled differences in the kinematic structure, as described below:

NE2 (Fig. 2a): Of the five slit positions shown in Figure 2, NE2 displays the most asymmetric structure, because the redshifted/NW polar lobe of the LH is essentially invisible. This implies that the NE2 slit position encounters more extinction in the equator than at other positions, blocking the light from the far side of the nebula. Indeed, this region located 2''-3'' north of the star is relatively dark in optical images and has a high optical depth of cool dust (Smith et al. 2003b). The only sign of the NW lobe is a faint blotch at $0~{\rm km~s^{-1}}$, +2'', which coincides with a feature in the equatorial skirt at visual wavelengths. This signifies that bright portions of the skirt may be holes where light can penetrate. The SE polar lobe is bright, and has a morphology consistent with a slice through a flattened polar bubble.

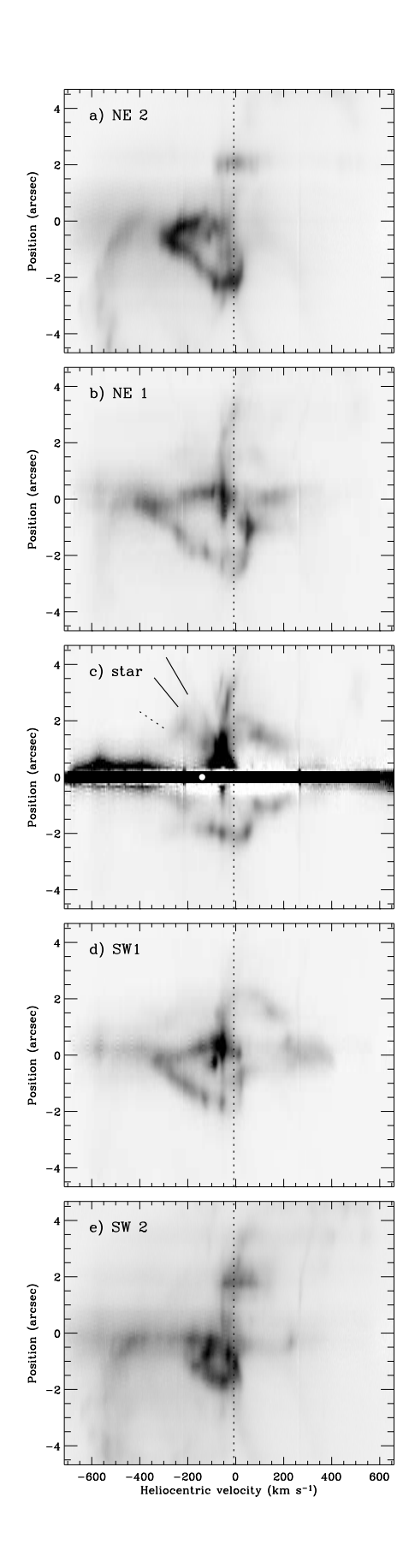


Figure 2. (a) Long-slit kinematics of [Fe II] $\lambda 16435$ around η Car at the five slit positions shown in Fig. 1. $V_{\rm sys}{=}-8.1$ km s⁻¹ (Smith 2004) is marked with a dashed line.

NE1 (Fig. 2b): The kinematic structure at this position already differs from NE2. Part of the redshifted NW lobe can be seen, although it still suffers more extinction than the blueshifted lobe. Here the SE lobe has a more angular or trapezoidal shape than at NE2, with straight side walls. pointed corners, and a flat polar cap. Velocities as fast as -400 km s⁻¹ are seen. An interesting feature at the NE1 position is the pair of bright spots that occupy the equator of the LH, giving the impression of a slice through a tilted equatorial ring (also seen in channel maps of [Fe II] $\lambda 4891$ presented by Ishibashi et al., and in gasdynamical simulations of the LH; Gonzalez et al. 2004). These are the kinematic counterparts of the Purple Haze and [S III] and [N II] features in images, which show marked temporal variability (Smith et al. 2000; 2004a). At the display scale chosen here (see §4), a line drawn through these two features would trace out an equatorial plane tilted from the plane of the sky by $\sim 40^{\circ}$, consistent with the inclination of the Homunculus (Smith 2002b; Davidson et al. 2001).

STAR (Fig. 2c): Both polar lobes of the LH are clearly seen at this position, indicating that here we can see to the far side of the LH (Smith et al. 1998; Smith & Gehrz 2000; Davidson et al. 2001; Smith 2002b). Interestingly, this is also the only slit position exhibiting blueshifted equatorial [Fe II] emission from the "skirt" of the Homunculus. The saturated stellar continuum makes it impossible to measure the precise velocity of the LH along the line of sight, but considering the kinematic structure in adjacent slit positions, the blueshifted wall of the LH crosses our line of sight to the star at -140 ± 20 km s⁻¹ (shown with the white dot). This agrees with the UV absorption component at -146 km s⁻¹ (Gull et al. 2004), confirming that the absorption feature is indeed from the LH. The bright [Fe II] emission just northwest of the star at -46 km s⁻¹ (Smith 2004) is from the Weigelt knots (Weigelt & Ebersberger 1986).

SW1 (Fig. 2d): The SW1 position gives the best representation of the bipolar structure of the LH, with two nearly complete, closed polar lobes. It exhibits the same flat-topped or trapezoidal structure as is seen at NE1. However, SW1 begins to show asymmetry in the LH; the redshifted NW lobe is about 20% larger than the SE lobe. Also, unlike NE1, there is a strong brightness asymmetry in the emission knots associated with the equatorial ring (the blueshifted knot is much brighter, as for the slit passing through the star).

SW2 (Fig. 2e): Structure at this position further accentuates the asymmetry of the LH. The blueshifted lobe is much smaller than its counterpart at NE2, and it is about half the size of its own redshifted lobe. Obscuration of the redshifted lobe by dust in the equator is apparent.

¹ This position also shows blueshifted He I $\lambda 10830$ (Smith 2002b), [Ni II] $\lambda 7379$ (Davidson et al. 2001), [Sr II] (Hartman et al. 2004), and narrow H91 α (Duncan et al. 1997). At least two different velocity components are seen here – a slow narrow component and a somewhat broader fast component at a different tilt angle (see also Hartman et al. 2004; Smith 2002b; Davidson et al. 2001). The two solid diagonal lines in Figure 2c are the tilt angles of the equator in these plots for ejection dates of 1843 and 1890, and the dashed line is for 1940. The narrow component lies close to the expected tilt for 1843, while the broader equatorial component seems to have been ejected after 1890 but well before 1940 (see Smith & Gehrz 1998; Dorland et al. 2004; Smith et al. 2004b).

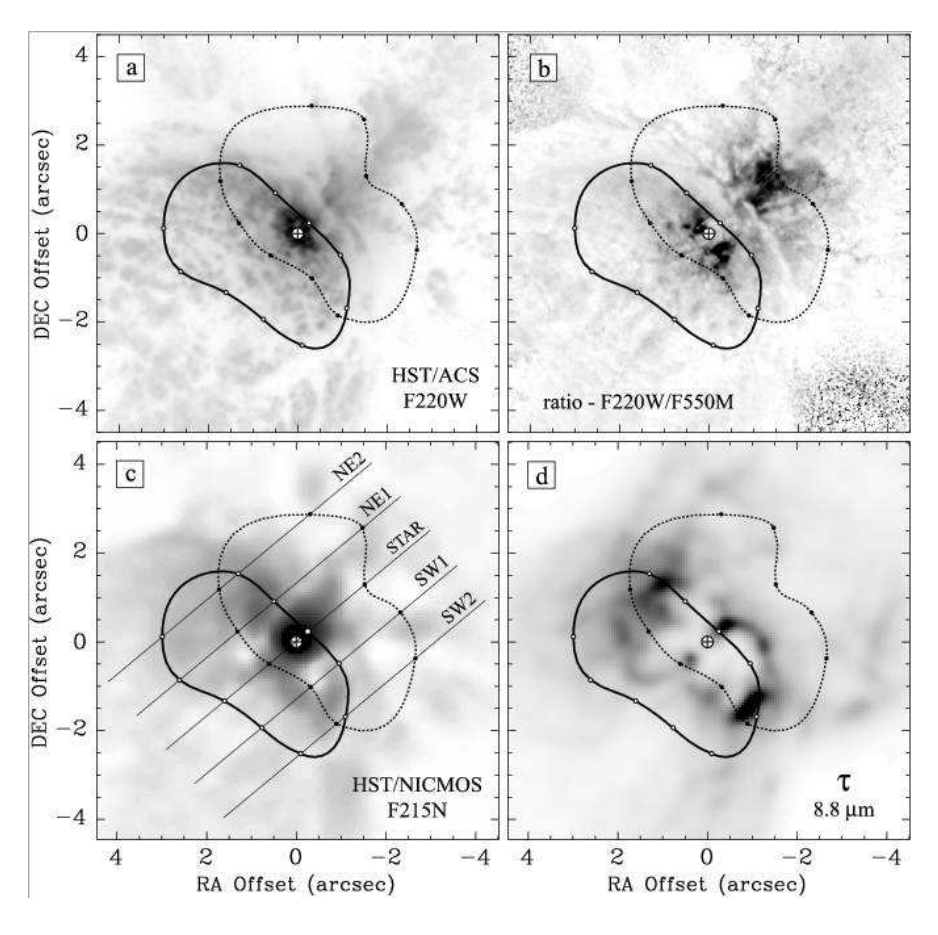


Figure 3. The spatial extents of the blueshifted (solid) and redshifted (dotted) polar lobes of the LH superposed on various images of η Car: (a) 2200 Å image (Smith et al. 2004b); (b) 2200 Å/5500 Å flux ratio image showing the UV excess emission from the "Purple Haze" (Smith et al. 2004b); (c) near-IR 2.15 μ m continuum image (Smith & Gehrz 2000); (d) 8.8 μ m optical depth or the column density of warm dust (Smith et al. 2003b). Filled and unfilled circles mark the measured extremities of the LH lobes along each of the five slit positions, while the curves are interpolated between these points.

4 THE AGE OF THE LITTLE HOMUNCULUS

The shape of the LH and the way its kinematic structure is displayed in Figure 2 can give valuable clues to its age. The relative scale between the spatial and velocity directions in Figure 2 reflects the age, in the sense that a horizontal stretch implies younger material, and horizontal compression implies older material. Since the LH has some inherent asymmetry, the choice of the horizontal stretch is subjective, depending on which features one uses to gauge the appropriate scaling. Figure 2 is displayed with a scale of $1^{\prime\prime}=117$ km s $^{-1}$, corresponding to an ejection date around 1910. This was chosen to match proper motions of the Weigelt knots (Smith et al. 2004a). Also, at this scale, a line drawn through the two bright equatorial knots at the NE1 position is tilted from vertical by $\sim\!40^\circ$, which matches the inclination of the Homunculus, as noted above.

However, at this display scale, some portions of the LH still appear somewhat stretched, which has two ramifications. First, if one assumes axial symmetry, it confirms that the Homunculus was not ejected during the Great Eruption in the 1840s, because such features would be horizontally compressed, rather than elongated. Second, the polar features look the most symmetric at a display scale corresponding to a later ejection date of 1920–1930.

The potential reconciliation of the age discrepancy may have to do with acceleration of ejecta, as suggested already by Smith et al. (2004b). Material ejected in the 1890 event that has been accelerated by radiation pressure or stellar wind ram pressure would show faster Doppler shifts and higher proper motion than expected. As noted already, equatorial zones of the LH have probably been accelerated since an 1890 ejection (Smith et al. 2004b). In Figure 2 the polar features appear elongated even for an ejection date of 1910 — if they originated in the 1890 event as well, they must have been accelerated even more than the corresponding equatorial features. In polar directions, ram pressure of the wind probably dominates, since η Car has a latitude-dependent wind with an effective mass-loss rate of $\dot{M} \simeq 10^{-3} M_{\odot} \text{ yr}^{-1}$ and polar speeds of 600 km s⁻¹ (Smith et al. 2003a). Thus, the polar wind speed is much faster than the LH, so we should expect some interaction. The fact that the polar caps of the LH have so far maintained their integrity means that the fast stellar wind has not been able to plow through the LH or disrupt it through Rayleigh-Taylor instabilities, so momentum is being transferred from the stellar wind to the LH. The acceleration depends on the mass of the LH, of course, which is investigated below in §6. In any case, the stretch of the polar caps indicates that

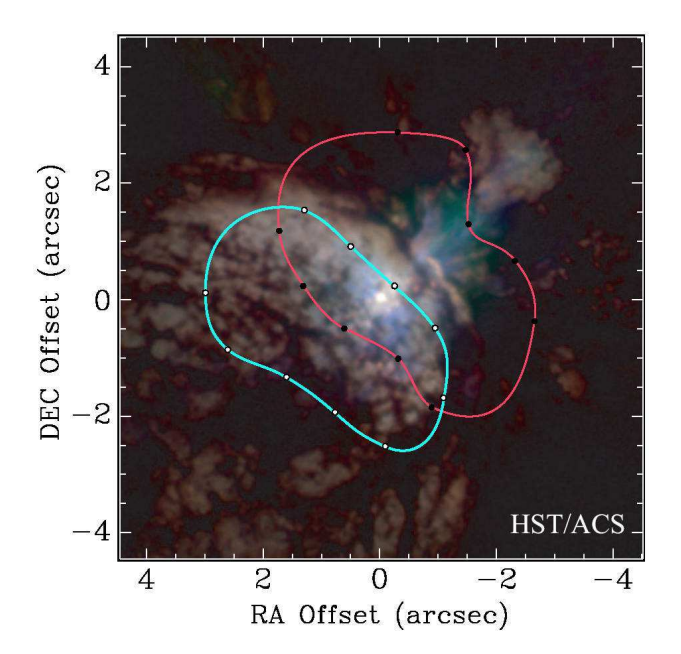


Figure 4. The spatial extents of the blueshifted (blue) and redshifted (red) polar lobes of the LH superposed on a 3-color HST/ACS image of η Car from Smith et al. (2004b)

the expansion of the LH is not perfectly homologous like its larger counterpart.

5 SPATIAL EXTENT

In lieu of a direct image of the LH, it is useful to investigate its projected appearance using spatial information gleaned from Figure 2. The measured extremeties of the blueshifted and redshifted polar lobes along each of the five slits are shown in Figures 3 and 4, superposed on various imaging data from previous studies. Obviously, some artistic license was taken in drawing these smooth curves, especially beyond the NE2 and SW2 slit positions where no additional information is available. Nevertheless, these curves give a fair depiction of the overall extent of the LH.

The LH has no outstanding correspondence with any of the clumps and filaments seen in scattered light in normal UV or visual-wavelength images of η Car, although it does match the spatial extent of the "Purple Haze" (Figs. 3a and 4). This correlation is most striking in Figure 3b, where the Purple Haze emission is almost entirely within the boundaries of the LH. The brightest UV excess within 1" to the NE and SW of the star is in the overlap region of the two polar lobes of the LH, where one expects to find the LH's equatorial features. At near-IR wavelengths where one sees through the dust in the SE polar lobe of the Homunculus, there is no correlation between the LH and scattered near-IR continuum light (Figure 3c).

It is quite evident from Figure 3d that the LH and the disrupted "dust torus" seen in the thermal-IR (Smith et al. 2002) are not the same physical structure, although there may be an interesting relationship between them. The NW edge of the blueshifted LH lobe and the SE edge of the redshifted lobe both seem to hug the inside edges of the dust torus. This implies that the dust torus is really an equatorial

ring, and would impede expansion of the LH at low latitudes, while the LH is free to expand out the poles. The distinct lack of dust in the interior regions supports the conjecture that the bright [Fe II] emission in the LH arises because Fe atoms are not locked up in grains.

Interestingly, the best spatial corresponce between the LH and features seen in images is with variable radio continuum structures (Duncan et al. 1997). The brightest radio continuum features are presumably equatorial, but the low-level contours of 3 cm emission coincide spatially with the extent of the LH. Furthermore, while the NW equatorial feature shows narrow blueshifted H91 α emission, the fainter surrounding emission shows broad lines with widths of ± 250 km s⁻¹ (Duncan et al. 1997). This velocity range agrees well with the kinematics of the LH.

6 MASS AND KINETIC ENERGY

6.1 Mass Estimate # 1: Density and Geometry

One way to estimate the mass of the LH is to simply deduce values for the volume and average density. Figure 2 indicates that the polar caps of the LH can be approximated as two disks, each with a radius of 1".6 (5.9×10¹⁶ cm) and thickness 0".4 (1.4×10¹⁶ cm). Thus, the volume occupied by the polar caps of the LH is roughly 3×10^{50} cm³ (this includes both poles). Approximating the side walls of the LH as a pair of truncated funnels with the same thickness gives roughly the same volume as contributed by the caps, for a total volume of $V \simeq 6\times10^{50}$ cm³. Then the mass of the LH is given by

$$M_{LH} = \mu m_H \frac{n_e}{\chi} f V \tag{1}$$

where $\mu \simeq 1.25$ for a He mass fraction Y=0.4, χ is the hydrogen ionization fraction, and f is a filling factor of ~ 0.5 .

Near-IR [Fe II] line ratios suggest an electron density of roughly $10^{4.2}$ cm⁻³ in the LH (Smith 2002b). However, given the presence of molecular hydrogen (Smith 2002b) and weakness of H α in the Homunculus, the ionization fraction in the LH is probably low, although not as low as in the more distant lobes of the Homunculus. Calculations with the CLOUDY spectral synthesis code intended to explain the ionization structure of the Homunculus give $\chi \simeq 10^{-3}$ at the inner edge of its [Fe II] zone (G. Ferland, private comm.). Much closer to the star in the Weigelt knots, χ rises to 0.5 (Verner et al. 2002). Thus, χ =0.05 is probably a reasonable intermediate value to choose for the LH, where the radiation field is more intense than in the Homunculus. With n_e = $10^{4.2}$, f=0.5, and χ =0.05, the total mass of the LH would be \sim 0.1 M_{\odot} .

6.2 Mass Estimate # 2: Inertia

Another way to deduce the mass of the LH is to ask how much inertia is needed to avoid excessive acceleration by the stellar wind over an assumed age t. For example, if the LH were too "light", η Car's powerful stellar wind would quickly accelerate the LH up to nearly 600 km s⁻¹, which would violate the LH's observed current expansion speed of \sim 250 km s⁻¹ (Fig. 2). The horizontal elongation of the polar regions of the LH in Figure 2 implies that the poles have been accelerated more than equatorial zones. This may

result from higher momentum flux in the polar wind (Smith et al. 2003a).

Under the assumption of acceleration by the ram pressure of a steady stellar wind ρv^2 , where $v = v_{\infty} - v$ is the relative velocity between η Car's polar wind and the changing speed of the LH, v = v(t), the equation of motion gives

$$\int \frac{dv}{(v_{\infty} - v)^2} = \frac{\dot{M}t}{mv_{\infty}} \tag{2}$$

where \dot{M} is η Car's average mass loss rate during this time, and m is the mass of a spherical shell accelerated by the wind. This can be integrated to yield a relation for the mass of the LH in terms of the initial ejection velocity of the LH, u, and the current observed difference between the stellar wind and the speed of the LH, $\Delta v = v_{\infty} - v_{LH}$, given by

$$M_{LH} = \frac{\Omega}{4\pi} f \dot{M} t \left[\frac{1 - u/v_{\infty}}{v_{\infty}/\Delta v - u/\Delta v - 1} \right]$$
 (3)

where Ω is the solid angle of the LH as seen by the star, and f is a filling factor or efficiency factor for the momentum transfer (i.e. $f \times \Omega/4\pi$ corrects for the fact that the LH is not a uniform spherical shell with mass m). From the observed geometry of the LH in Figure 2, $\Omega \simeq 2\times 2$ ster. Furthermore, from observations we can adopt $\dot{M}=10^{-3}M_{\odot}$ yr⁻³, $v_{\infty}=600$ km s⁻¹ (e.g., Hillier et al. 2001), and a present value for the polar speed of the LH of $v_{LH}=250$ km s⁻¹, so that $\Delta v = v_{\infty} - v_{LH} = 350$ km s⁻¹. Then, the remaining quantities are t, u, and M_{LH} .

In the most plausible scenario, where the LH was ejected in the 1890 event, we have t=114 yr. Furthermore, spectra obtained in 1893 showed absorption features at about -200 km s⁻¹ (Walborn & Liller 1977; Whitney 1952), which gives a plausible value for u. With these constraints, equation (3) gives $M_{LH} = f \times 0.17 \, M_{\odot}$. The similar values in methods 1 and 2 are somewhat misleading, since method 2 only applies to the polar region (about 1/2 of the mass). In any case, these arguments suggest that the likely mass of the LH is of order $0.1-0.2 \, M_{\odot}$. This is consistent with the lower mass estimated by Ishibashi et al. (2003).

This rough agreement between the two independent mass estimates is encouraging, and adds additional support for an 1890 ejection and subsequent acceleration of the LH by the 20th-century stellar wind. If the LH was ejected after 1890 or if the acceleration has not been constant, then the problem obviously becomes more difficult. The alternative scenario – where the LH and the Weigelt knots were instead ejected in the early 20th century (Smith et al. 2004b; Dorland et al. 2004; Ishibashi et al. 2003) – seems less likely. Higher masses are required if the LH was ejected after 1890, because it would need to more effectively resist acceleration. For example, for an ejection date of 1930 and only 1% acceleration, the required mass is about 1 M_{\odot} (with the same filling factor f=0.5). Masses much above 0.1 M_{\odot} begin to seem highly implausible, since the LH is invisible in images and has not formed large quantities of dust. In other words, the present day expansion speed of the LH rules out an ejection date as late as 1940.

6.3 Kinetic Energy and the 1890 Outburst

With a mass of $0.1-0.2~M_{\odot}$ in the LH, Doppler shifts allow one to estimate the kinetic energy released in the 1890 event.

Most of the kinetic energy will be contained in the $\sim 0.1~M_{\odot}$ of material in the two polar caps of the LH, moving at 250 km s⁻¹, while a small fraction is contributed by mass in the side walls moving at slower speeds. Then, the total kinetic energy released in the 1890 event is about $10^{46.9}$ ergs.

This is a factor of 500 less kinetic energy than was expelled in the Great Eruption (Smith et al. 2003b), signifying that the ultimate sources of energy for the 1890 and 1840's events were very different. Furthermore, averaged over the 7 yr duration of the 1890 outburst (Humphreys et al. 1999), the mass-loss rate was $\dot{M} \simeq 0.02~M_{\odot}$. This was only $\sim 4\%$ of that during the Great Eruption, and the momentum imparted to the 1890 ejecta was only about 1-2% of that during the larger event. Finally, in the 1890 event the ratio of mechanical-to-radiative luminosity was about 0.02, compared to numbers closer to unity for the Great Eruption itself (here I have assumed that the bolometric radiative luminosity was a constant 5×10^6 L_{\odot} during the 1890 event, whereas it increased by about a factor of 4-5 in the 1840's; Humphreys et al. 1999). Thus, the physics of the mass ejection was also quite different in the two 19th century outbursts.

It is also instructive to compare the 1890 event with the present-day stellar wind of η Carinae. The average massloss rate of the 1890 event was about 20 times higher than the present-day stellar wind, while the wind momentum was about 10 times stronger. Thus, the 1890 event was indeed an outburst, in the sense that the mass loss was enhanced compared to the normal stellar wind parameters. Interestingly, however, the ratio of mechanical-to-radiative luminosity in 1890 was about 2% – only slightly more than the value for the present-day stellar wind – so the acceleration of the LH used up a similar fraction of available luminosity. In a radiatively driven wind, it is often useful to know the wind's "performance number" (the ratio of wind momentum to photon momentum), given by

$$\zeta = \frac{\dot{M} \, v}{L/c} \tag{4}$$

where $L \simeq 5 \times 10^6~L_{\odot}$ is the radiative luminosity during the 1890 event. Thus, $\zeta_{1890} \simeq 50$, while for the present day stellar wind $\zeta \simeq 5$ (note that $\zeta \gtrsim 10^3$ during the Great Eruption; Smith et al. 2003b). Performance numbers as high as ~ 10 are typically expected for very dense line-driven winds (Lucy & Abbott 1993; Springmann & Puls 1998), so if mass-loss during the 1890 outburst was a line-driven wind, it was certainly pushing the limits of that acceleration mechanism.

7 SUMMARY: PERSISTENTLY BIPOLAR

The main results of this study are the following:

1. The kinematic structure of the LH would seem to suggest ejection dates between 1910 and 1930 if one assumes linear expansion and rough axial symmetry. However, linear expansion may be an invalid assumption: the polar caps of the LH appear to be intact, suggesting that the faster posteruption wind has not yet broken through the LH and may be accelerating it. Thus, even though the expansion of the LH is non-homologous, it may all have been ejected during the 1890 eruption if it has been accelerated by ram pressure

of the post-eruption wind. In this case, the polar caps of the LH have been accelerated more than low-latitudes.

2. Various clues indicate a total mass for the LH of roughly $0.1~M_{\odot}$, so the kinetic energy released in the 1890 event was roughly $10^{46.9}$ ergs. Thus, the 1890 event was orders-of-magnitude less powerful than the Great Eruption in the 1840's, indicating that the two events had a different energy source and probably a different root cause.

Despite these differences, both eruptions gave rise to similar bipolar geometry with the same polar axis. This may point toward an external collimation mechanism. For example, while internal processes may have brought about η Car's phenomenal energy release and mass ejection during the 1840's and again 50 years later, something else may have helped to collimate the outflow. η Car is thought to be a close binary system (Damineli et al. 2000), so one can certainly envision a scenario where the two stars interact violently during close periastron passages. This is by no means a new suggestion (e.g., Innes 1914), but difficult 3-D calculations are needed to proceed beyond mere speculation.

In this regard, however, it is interesting to note that some planetary nebulae surrounding symbiotic binary stars have nested bipolar nebulae that remind one of the LH and Homunculus of η Car. Two salient examples are Hb 12 (Hora et al. 2000; Welch et al. 1999) and He 2-104 (Corradi et al. 2001). Hb 12 is particularly interesting in that the smaller bipolar nebula has [Fe II] $\lambda 16435$ emission, while the larger bipolar shell emits near-IR lines of molecular hydrogen (Welch et al. 1999), just like the LH and Homunculus around η Car (Smith 2002b). Of course, the fact that these symbiotic planetary nebulae have also had sporadic outbursts with the same recurring bipolar geometry does not mean that they share the same collimation mechanism as η Car, but the nebular similarities are intriguing.

On the other hand, the present-day stellar wind is also bipolar and shares the same axis as the Homunculus (Smith et al. 2003a). Thus, some intrinsic mechanism that persistently sends material poleward may be at work in η Car as well (e.g., Owocki & Gayley 1997; Matt & Balick 2004).

ACKNOWLEDGMENTS

Support was provided by NASA through grant HF-01166.01A from the Space Telescope Science Institute, which is operated by the Association of Universities for Research in Astronomy (AURA), Inc., under NASA contract NAS 5-26555. These data were obtained in service observing mode, and I thank the Gemini staff for their assistance.

REFERENCES

Boumis, P., Meaburn, J., Bryce, M., & Lopez, J.A. 1998, MNRAS, 294, 61

Corradi, R.L.M., Livio, M., Balick, B., Munari, U., & Schwarz, H.E. 2001, ApJ, 553, 211

Currie, D.G., et al. 1996, AJ, 112, 1115

Damineli, A., Kaufer, A., Wolf, B., Stahl, O., Lopes, D.F., & de Araújo, F.X. 2000, ApJ, 528, L101

Davidson, K., Smith, N., Gull, T.R., Ishibashi, K., & Hillier, D.J. 2001, AJ, 121, 1569

Dorland, B.N., Currie, D.G., & Hajian, A.R. 2004, AJ, 127, 1052
Duncan, R.A., White, S.M., Reynolds, J.E., & Lim, J. 1997, in
ASP Conf. Ser. 179, Eta Carinae at the Millenium, eds. J.A.
Morse, R.M. Humphreys, & A. Damineli (san Francisco: ASP),

Frank, A., Balick, B., & Davidson, K. 1995, ApJ, 441, L77

Frank, A., Ryu, D., & Davidson, K. 1998, ApJ, 500, 291

Garcia-Segura, G., Langer, N., & MacLow, M.M. 1997, in ASP Conf. Ser. 120, Luminous Blue Variables: Massive Stars in Trabsition, ed. A. Nota & H.J.G.L.M. Lamers (san Francisco: ASP), 332

Gonzalez, R., de Gouveia Dal Pino, E.M., Raga, A.C., & Velazquez, P.F. 2004, ApJ, 600, L59

Gull, T.R., et al. 2004, submitted

Hartman, H., Gull, T.R., Johansson, S., Smith, N., & the HST Eta Car Treasury Project Team 2004, A&A, 419, 215

Hillier, D.J., Davidson, K., Ishibashi, K., & Gull, T.R. 2001, ApJ, 553, 837

Hinkle, K.H., Blum, R., Joyce, R.R., Ridgeway, S.T., Rodgers, B., Sharp, N., Smith, V., Valenti, J., & van der Bliek, N. 2003, Proc. SPIE 4834, 353

Hora, J.L., et al. 2000, in ASP Conf. Ser. 199, Asymmetrical Planetary Nebulae II: From Origins to Microstructures, eds. J.H. Kastner, N. Soker, & S. Rappaport (San Francisco: ASP), 267

Humphreys, R.M., Davidson, K., & Smith, N. 1999, PASP, 111, 1124

Innes, R.T.A. 1914, MNRAS, 74, 697

Ishibashi, K., et al. 2003, AJ, 125, 3222

Langer, N., Garcia-Segura, G., & MacLow, M.M. 1999, ApJ, 520, L49

Lucy, L.B., & Abbott, D.C. 1993, ApJ, 405, 738

Maeder, A., & Desjacques, V. 2001, A&A, 372, L9

Matt, S., & Balick, B. 2004, ApJ, 615, 921

Morse, J.A., Kellogg, J.R., Bally, J., Davidson, K., Balick, B., & Ebbets, D. 2001, ApJ, 548, L207

Owocki, S.P., & Gayley, K.G. 1997, in ASP Conf. Ser. 120, Luminous Blue Variables: Massive Stars in Trabsition, ed. A. Nota & H.J.G.L.M. Lamers (san Francisco: ASP), 121

Smith, N. 2002a, MNRAS, 336, L22

Smith, N. 2002b, MNRAS, 337, 1252

Smith, N. 2004, MNRAS, 351, L15

Smith, N., Davidson, K., Gull, T.R., Ishibashi, K., & Hilier, D.J. 2003a, ApJ, 586, 432

Smith, N., & Gehrz, R.D. 1998, AJ, 116, 823

Smith, N., & Gehrz, R.D. 2000, ApJ, 529, L99

Smith, N., Gehrz, R.D., & Krautter, J. 1998, AJ, 116, 1332

Smith, N., Gehrz, R.D., Hinz, P.M., Hoffmann, W.F., Mamajek, E.E., Meyer, M.R., & Hora, J.L. 2002, ApJ, 567, L77

Smith, N., Gehrz, R.D., Hinz, P.M., Hoffmann, W.F., Hora, J.L., Mamajek, E.E., & Meyer, M.R. 2003b, AJ, 125, 1458

Smith, N., Morse, J.A., Davidson, K., & Humphreys, R.M. 2000, A.J. 120, 920

Smith, N., Morse, J.A., Collins, N.R., & Gull, T.R. 2004a, ApJ, 610, L105

Smith, N., et al. 2004b, ApJ, 605, 405

Soker, N. 2004, ApJ, 612, 1060

Springmann, U., & Puls, J. 1998, in ASP Conf. Ser. 131, Boulder-Munich II: Properties of Hot Luminous Stars, ed. I.D. Howarth (San Francisco: ASP), 286

Verner, E.M., Gull, T.R., Bruhweiler, F., Johansson, S., Ishibashi, K., & Davidson, K. 2002, ApJ, 581, 1154

Walborn, N.R., & Liller, M. 1977, ApJ, 211, 181

Weigelt, G., & Ebersberger, J. 1986, A&A, 163, L5

Welch, C.A., Frank, A., Pipher, J.L., Forrest, W.J., & Woodward, C.E. 1999, ApJ, 522, L69

Whitney, C.A. 1952, Harvard Obs. Bull., 921, 8